Plasma broadening and shifting of spectral lines along the isoelectronic sequence of boron

B. Blagojević, M. V. Popović, and N. Konjević
Institute of Physics, 11080 Belgrade, P.O. Box 68, Yugoslavia

M. S. Dimitrijević
Astronomical Observatory, 11050 Belgrade, Volgina 7, Yugoslavia

(Received 13 October 1995; revised manuscript received 28 February 1996)

Temperature dependence of the Stark widths (N III and F V) and shifts (N III and O IV) of the $3s^2S$-$3p(^1S)^2P^0$ and $3p^2P^0$-$3d(^1S)^2D$ transitions have been studied theoretically using the impact semiclassical method and experimentally observed in the plasma of a low pressure pulsed arc. Plasma electron densities were determined from the width of the He II P_α line while electron temperatures were measured from the relative line intensities. To estimate the influence of different ions on the width and shift of lines, evaluations of the plasma composition data were performed and, in conjunction with our theoretical results, the contribution of ion broadening was estimated. Within the estimated uncertainties experimental Stark widths agree well with the results of our semiclassical electron impact widths in the studied electron temperature range. For the conditions of the present experiment, estimated contribution of the ion broadening has never exceeded five percent of the total width. So within the precision of this experiment it was not possible to detect its presence with certainty. Along the boron isoelectronic sequence the experimental widths and shifts agree with semiclassical electron impact data predictions. In the case of O IV lines the inclusion of *the energy levels with different parent terms* in our semiclassical calculations of the Stark widths and shifts improved the agreement between theory and experiment considerably. Comparisons of the experimental widths with simple theoretical formulas for estimation of plasma broadened linewidths show an agreement within estimated uncertainties. [S1063-651X(96)00307-8]

PACS number(s): 52.70.Kz, 32.70.Jz

I. INTRODUCTION

Knowledge of the Stark width and shift dependence upon the temperature of the charged perturbers in the plasma is of importance for testing of the theory and for the reliable diagnostics of laboratory and astrophysical plasmas. Namely, the dependence of the Stark broadening parameters upon the electron concentration N_e has been tested in a number of experiments (see, e.g., Refs. [1] and [2] and references therein) while the dependence of these parameters upon the electron temperature T_e in a wider temperature range is tested only in a few cases. Usually, experimental results are reported for a single electron temperature and in most of the cases when comparison with another experiment is performed, temperature dependence of the Stark broadening parameter is neglected. This is justified by assuming weak dependence of the width w and shift d upon electron temperature T_e. This assumption may be used only in a small temperature range whose magnitude depends upon the shape of $w(T_e)$ and $d(T_e)$ curves (see, e.g., comparison between experimental and theoretical results in Figs. 1–4). Furthermore, the usual assumption that, in comparison with the electron impact contribution to the width or shift of ionized atom lines, one can neglect the contribution of ions, may not be correct (see, e.g., theoretical results for widths and shifts of O IV lines in Ref. [3] and Table I). This ion contribution may change the Stark broadening parameters and maybe temperature dependence at elevated temperatures. To answer quantitatively the above questions both theoretical and experimental study of the plasma broadened spectral line parameters of multiply ionized atoms are required.

Here, we present the results of experimental and theoretical study of the broadening and shift of the analogous transitions along the isoelectronic sequence of boron. These type of studies, which are very convenient for the testing of theory (similar energy level structure of the emitter with gradual increase of the ionic charge), also enables determination of the Stark width and/or shift dependence upon spectroscopic charge number Z of the emitter. This also is of importance for the estimation of the broadening parameters for the ions with no available data. An early study of the experimental line widths along isoelectronic sequence was performed in [4]. Although the analysis was based only on the few experimental data it was clearly demonstrated that the widths decrease strongly with increasing ionic charge [4]. Since then several publications have reported experimental measurements of the Stark widths and shifts of the analogous transitions along isoelectronic sequences [5–8]. In all the experiments gradual decrease of the Stark widths with an increase of Z is detected. A Z^{-1} scaling of the Stark widths was found for $3s-3p$ transitions in Li-like ions (up to $Z=6$) [5]. In another experiment this study is extended to higher ionized species (up to $Z=8$) and systematic deviations of the line widths from the theoretically expected Z^{-2} scaling is detected [7]. In a recent experiment [8] along boron isoelectronic sequence, $3s$-$3p$ and $3p$-$3d$ transitions, considerable widths deviations are detected for $Z=5$ and $Z=6$ from those predicted by some theoretical calculations. Recent experimental studies of the Stark shifts of the $4s$-$4p$ transition along the P isoelectronic sequence (S II, Cl III, and Ar IV) also showed a gradual decrease of shifts with increase of Z [6] (see also [9]). Furthermore, the change of the sign of the

TABLE I. This table shows Stark broadening parameters for the $3s^2S$-$3p(^1S)^2P^0$ and the $3p^2P^0$-$3d(^1S)^2D$ multiplets of *N* III, *O* IV, and *F* V for the perturber density of 10^{17} cm^{-3} and temperatures from 10 000 up to 300 000 K. Transition and averaged wavelengths for the multiplet in Å are also given. If one divides the *C* value by the Stark width value, we obtain an estimate for the maximum perturber density (in cm^{-3}) for which the line may be treated as isolated and the tabulated data may be used. Brackets in the table enclose powers of ten.

Perturber density$=1\times10^{17}$ cm^{-3}					
Perturbers are:		Electrons		Protons	
Transition	T (K)	Width (Å)	Shift (Å)	Width (Å)	Shift (Å)
N III $3s$-$3p$	10 000	0.474	0.116[−02]	0.388[−02]	−0.131[−02]
4100.5 Å	20 000	0.339	−0.682[−02]	0.786[−02]	−0.268[−02]
$C=0.36E+21$	30 000	0.283	−0.743[−02]	0.105[−01]	−0.370[−02]
	50 000	0.231	−0.625[−02]	0.137[−01]	−0.506[−02]
	100 000	0.183	−0.832[−02]	0.168[−01]	−0.697[−02]
	150 000	0.162	−0.742[−02]	0.183[−01]	−0.773[−02]
N III $3p$-$3d$	10 000	0.584	−0.827[−02]	0.101[−01]	−0.409[−02]
4639.9 Å	20 000	0.424	−0.857[−02]	0.229[−01]	−0.916[−02]
$C=0.46E+21$	30 000	0.355	−0.752[−02]	0.325[−01]	−0.132[−01]
	50 000	0.290	−0.688[−02]	0.436[−01]	−0.191[−01]
	100 000	0.229	−0.940[−02]	0.586[−01]	−0.268[−01]
	150 000	0.205	−0.764[−02]	0.641[−01]	−0.304[−01]
Perturbers are:		He II		He III	
N III $3s$-$3p$	10 000	0.597[−02]	−0.129[−02]	0.710[−02]	−0.232[−02]
4100.5 Å	20 000	0.103[−01]	−0.253[−02]	0.149[−01]	−0.512[−02]
$C=0.36E+21$	30 000	0.127[−01]	−0.344[−02]	0.203[−01]	−0.725[−02]
	50 000	0.156[−01]	−0.466[−02]	0.267[−01]	−0.102[−01]
	100 000	0.178[−01]	−0.583[−02]	0.334[−01]	−0.142[−01]
	150 000	0.191[−01]	−0.649[−02]	0.364[−01]	−0.158[−01]
N III $3p$-$3d$	10 000	0.129[−01]	−0.225[−02]	0.163[−01]	−0.406[−02]
4639.9 Å	20 000	0.205[−01]	−0.427[−02]	0.317[−01]	−0.878[−02]
$C=0.46E+21$	30 000	0.252[−01]	−0.570[−02]	0.403[−01]	−0.123[−01]
	50 000	0.288[−01]	−0.737[−02]	0.520[−01]	−0.166[−01]
	100 000	0.327[−01]	−0.929[−02]	0.617[−01]	−0.230[−01]
	150 000	0.350[−01]	−0.104[−01]	0.665[−01]	−0.256[−01]
Perturbers are:		N II		N III	
N III $3s$-$3p$	10 000	0.753[−02]	−0.127[−02]	0.963[−02]	−0.231[−02]
4100.5 Å	20 000	0.118[−01]	−0.240[−02]	0.183[−01]	−0.495[−02]
$C=0.36E+21$	30 000	0.143[−01]	−0.319[−02]	0.231[−01]	−0.692[−02]
	50 000	0.162[−01]	−0.410[−02]	0.296[−01]	−0.927[−02]
	100 000	0.184[−01]	−0.516[−02]	0.348[−01]	−0.127[−01]
	150 000	0.197[−01]	−0.576[−02]	0.374[−01]	−0.142[−01]
N III $3p$-$3d$	100 000	0.160[−01]	−0.220[−02]	0.214[−01]	−0.402[−02]
4639.9 Å	20 000	0.236[−01]	−0.407[−02]	0.372[−01]	−0.838[−02]
$C=0.46E+21$	30 000	0.274[−01]	−0.520[−02]	0.461[−01]	−0.116[−01]
	50 000	0.303[−01]	−0.675[−02]	0.559[−01]	−0.154[−01]
	100 000	0.340[−01]	−0.832[−02]	0.638[−01]	−0.203[−01]
	150 000	0.358[−01]	−0.921[−02]	0.684[−01]	−0.226[−01]
Perturbers are:		N IV		N V	
N III $3s$-$3p$	10 000	0.103[−01]	−0.305[−02]	0.102[−01]	−0.354[−02]
4100.5 Å	20 000	0.222[−01]	−0.732[−02]	0.251[−01]	−0.952[−02]
$C=0.36E+21$	30 000	0.304[−01]	−0.105[−01]	0.359[−01]	−0.141[−01]
	50 000	0.400[−01]	−0.149[−01]	0.485[−01]	−0.210[−01]
	100 000	0.501[−01]	−0.211[−01]	0.656[−01]	−0.301[−01]
	150 000	0.546[−01]	−0.237[−01]	0.718[−01]	−0.345[−01]
N III $3p$-$3d$	10 000	0.236[−01]	−0.534[−02]	0.239[−01]	−0.620[−02]
4639.9 Å	20 000	0.471[−01]	−0.126[−01]	0.538[−01]	−0.164[−01]

TABLE I. (*Continued*.)

Perturber density=1×10^{17} cm^{-3}					
Perturbers are:		Electrons		Protons	
Transition	T (K)	Width (Å)	Shift (Å)	Width (Å)	Shift (Å)
$C=0.46E+21$	30 000	0.603[−01]	−0.178[−01]	0.731[−01]	−0.238[−01]
	50 000	0.779[−01]	−0.243[−01]	0.965[−01]	−0.343[−01]
	100 000	0.925[−01]	−0.341[−01]	0.120	−0.490[−01]
	150 000	0.997[−01]	−0.383[−01]	0.130	−0.550[−01]
Perturbers are:		N VI		N VII	
N III $3s$-$3p$	10 000	0.976[−02]	−0.385[−02]	0.962[−02]	−0.416[−02]
4100.5 Å	20 000	0.271[−01]	−0.115[−01]	0.284[−01]	−0.133[−01]
$C=0.36E+21$	30 000	0.399[−01]	−0.177[−01]	0.434[−01]	−0.211[−01]
	50 000	0.568[−01]	−0.268[−01]	0.647[−01]	−0.328[−01]
	100 000	0.802[−01]	−0.393[−01]	0.938[−01]	−0.490[−01]
	150 000	0.882[−01]	−0.463[−01]	0.105	−0.580[−01]
N III $3p$-$3d$	10 000	0.231[−01]	−0.675[−02]	0.230[−01]	−0.730[−02]
4639.9 Å	20 000	0.591[−01]	−0.199[−01]	0.631[−01]	−0.230[−01]
$C=0.46E+21$	30 000	0.838[−01]	−0.298[−01]	0.920[−01]	−0.357[−01]
	50 000	0.112	−0.442[−01]	0.126	−0.543[−01]
	100 000	0.147	−0.644[−01]	0.174	−0.803[−01]
	150 000	0.161	−0.737[−01]	0.191	−0.924[−01]
Perturbers are:		Electrons		Protons	
O IV $3s$-$3p$	10 000	0.299	0.188[−01]	0.407[−03]	0.288[−04]
3066.4 Å	20 000	0.198	0.171[−01]	0.107[−02]	0.648[−04]
$C=0.28E+21$	30 000	0.155	0.129[−01]	0.173[−02]	0.100[−03]
	50 000	0.121	0.104[−01]	0.276[−02]	0.170[−03]
	100 000	0.903[−01]	0.803[−02]	0.416[−02]	0.322[−03]
	150 000	0.776[−01]	0.650[−02]	0.501[−02]	0.433[−03]
O IV $3p$-$3d$	10 000	0.278	0.174[−01]	0.910[−03]	0.222[−03]
3410.9 Å	20 000	0.177	0.147[−01]	0.230[−02]	0.499[−03]
$C=0.34E+21$	30 000	0.144	0.110[−01]	0.356[−02]	0.762[−03]
	50 000	0.112	0.871[−02]	0.542[−02]	0.122[−02]
	100 000	0.824[−01]	0.737[−02]	0.782[−02]	0.199[−02]
	150 000	0.701[−01]	0.643[−02]	0.896[−02]	0.240[−02]
Perturbers are:		He III		O III	
O IV $3s$-$3p$	10 000	0.722[−03]	0.475[−04]	0.112[−02]	0.475[−04]
3066.4 Å	20 000	0.199[−02]	0.121[−03]	0.289[−02]	0.121[−03]
$C=0.28E+21$	30 000	0.325[−02]	0.193[−03]	0.442[−02]	0.193[−03]
	50 000	0.528[−02]	0.334[−03]	0.663[−02]	0.331[−03]
	100 000	0.810[−02]	0.643[−03]	0.944[−02]	0.620[−03]
	150 000	0.982[−02]	0.875[−03]	0.107[−01]	0.831[−03]
O IV $3p$-$3d$	10 000	0.162[−02]	0.367[−03]	0.247[−02]	0.367[−03]
3410.9 Å	20 000	0.429[−02]	0.933[−03]	0.602[−02]	0.930[−03]
$C=0.34E+21$	30 000	0.674[−02]	0.147[−02]	0.880[−02]	0.145[−02]
	50 000	0.104[−01]	0.241[−02]	0.124[−01]	0.231[−02]
	100 000	0.152[−01]	0.401[−02]	0.171[−01]	0.364[−02]
	150 000	0.177[−01]	0.487[−02]	0.186[−01]	0.445[−02]
Perturbers are:		O IV		O V	
O IV $3s$-$3p$	10 000	0.104[−02]	0.573[−04]	0.977[−03]	0.645[−04]
3066.4 Å	20 000	0.309[−02]	0.171[−03]	0.317[−02]	0.231[−03]
$C=0.28E+21$	30 000	0.504[−02]	0.279[−03]	0.540[−02]	0.359[−03]
	50 000	0.814[−02]	0.493[−03]	0.924[−02]	0.645[−03]
	100 000	0.124[−01]	0.959[−03]	0.150[−01]	0.130[−02]
	150 000	0.149[−01]	0.130[−02]	0.184[−01]	0.179[−02]
O IV $3p$-$3d$	10 000	0.232[−02]	0.442[−03]	0.219[−02]	0.498[−03]
3410.9 Å	20 000	0.664[−02]	0.131[−02]	0.693[−02]	0.164[−02]

TABLE I. *(Continued.)*

Perturber density $=1\times10^{17}$ cm^{-3}					
Perturbers are:		Electrons		Protons	
Transition	T (K)	Width (Å)	Shift (Å)	Width (Å)	Shift (Å)
$C=0.34E+21$	30 000	0.104[−01]	0.212[−02]	0.114[−01]	0.274[−02]
	50 000	0.160[−01]	0.355[−02]	0.185[−01]	0.471[−02]
	100 000	0.232[−01]	0.593[−02]	0.281[−01]	0.830[−02]
	150 000	0.268[−01]	0.724[−02]	0.340[−01]	0.101[−01]
Perturbers are:		O VI		C III	
O IV $3s$-$3p$	10 000	0.915[−03]	0.675[−04]	0.104[−02]	0.475[−04]
3066.4 Å	20 000	0.318[−02]	0.249[−03]	0.272[−02]	0.121[−03]
$C=0.28E+21$	30 000	0.561[−02]	0.434[−03]	0.421[−02]	0.193[−03]
	50 000	0.100[−01]	0.793[−03]	0.641[−02]	0.332[−03]
	100 000	0.174[−01]	0.162[−02]	0.923[−02]	0.625[−03]
	150 000	0.214[−01]	0.229[−02]	0.106[−01]	0.839[−03]
O IV $3p$-$3d$	10 000	0.206[−02]	0.521[−03]	0.231[−02]	0.367[−03]
3410.9 Å	20 000	0.703[−02]	0.192[−02]	0.571[−02]	0.931[−03]
$C=0.34E+21$	30 000	0.120[−01]	0.333[−02]	0.844[−02]	0.145[−02]
	50 000	0.204[−01]	0.586[−02]	0.121[−01]	0.233[−02]
	100 000	0.327[−01]	0.105[−01]	0.169[−01]	0.371[−02]
	150 000	0.403[−01]	0.133[−01]	0.185[−01]	0.454[−02]
Perturbers are:		C IV		C V	
O IV $3s$-$3p$	10 000	0.963[−03]	0.573[−04]	0.906[−03]	0.645[−04]
3066.4 Å	20 000	0.290[−02]	0.171[−03]	0.296[−02]	0.213[−03]
$C=0.28E+21$	30 000	0.477[−02]	0.279[−03]	0.508[−02]	0.359[−03]
	50 000	0.781[−02]	0.494[−03]	0.883[−02]	0.645[−03]
	100 000	0.120[−01]	0.963[−03]	0.146[−01]	0.130[−02]
	150 000	0.146[−01]	0.132[−02]	0.180[−01]	0.181[−02]
O IV 3p-3d	10 000	0.215[−02]	0.442[−03]	0.204[−02]	0.498[−03]
3410.9 Å	20 000	0.625[−02]	0.131[−02]	0.649[−02]	0.164[−02]
$C=0.34E+21$	30 000	0.990[−02]	0.212[−02]	0.108[−01]	0.275[−02]
	50 000	0.154[−01]	0.357[−02]	0.177[−01]	0.473[−02]
	100 000	0.227[−01]	0.602[−02]	0.274[−01]	0.839[−02]
	150 000	0.265[−01]	0.733[−02]	0.334[−01]	0.103[−01]
Perturbers are:		Electrons		Protons	
F V $3s$-$3p$	10 000	0.124	0.151[−01]	0.685[−04]	−0.756[−04]
2455.0 Å	30 000	0.658[−01]	−0.536[−05]	0.353[−03]	−0.277[−03]
$C=0.22E+21$	50 000	0.514[−01]	−0.840[−03]	0.684[−03]	−0.464[−03]
	100 000	0.375[−01]	−0.863[−03]	0.135[−02]	−0.817[−03]
	200 000	0.283[−01]	−0.102[−02]	0.207[−02]	−0.120[−02]
	300 000	0.243[−01]	−0.106[−02]	0.250[−02]	−0.147[−02]
F V $3p$-$3d$	10 000	0.129	−0.773[−02]	0.145[−03]	−0.830[−04]
2701.6 Å	30 000	0.758[−01]	−0.140[−02]	0.716[−03]	−0.304[−03]
$C=0.27E+21$	50 000	0.594[−01]	−0.914[−03]	0.131[−02]	−0.511[−03]
	100 000	0.433[−01]	−0.686[−03]	0.237[−02]	−0.908[−03]
	200 000	0.324[−01]	−0.101[−02]	0.342[−02]	−0.135[−02]
	300 000	0.279[−01]	−0.859[−03]	0.390[−02]	−0.165[−02]
Perturbers are:		He II		He III	
F V $3s$-$3p$	10 000	0.127[−03]	−0.756[−04]	0.118[−03]	−0.115[−03]
2455.0 Å	30 000	0.596[−03]	−0.275[−03]	0.661[−03]	−0.524[−03]
$C=0.22E+21$	50 000	0.102[−02]	−0.450[−03]	0.130[−02]	−0.905[−03]
	100 000	0.169[−02]	−0.759[−03]	0.262[−02]	−0.163[−02]
	200 000	0.236[−02]	−0.107[−02]	0.406[−02]	−0.244[−02]
	300 000	0.258[−02]	−0.125[−02]	0.495[−02]	−0.299[−02]
F V $3p$-$3d$	10 000	0.268[−03]	−0.830[−04]	0.250[−03]	−0.126[−03]

TABLE I. (*Continued*.)

Perturber density=1×10^{17} cm^{-3}					
Perturbers are:		Electrons		Protons	
Transition	T (K)	Width (Å)	Shift (Å)	Width (Å)	Shift (Å)
2701.6 Å	30 000	0.117[-02]	−0.302[−03]	0.134[−02]	−0.576[−03]
$C=0.27E+21$	50 000	0.189[−02]	−0.497[−03]	0.250[−02]	−0.997[−03]
	100 000	0.290[−02]	−0.845[−03]	0.462[−02]	−0.182[−02]
	200 000	0.381[−02]	−0.120[−02]	0.672[−02]	−0.274[−02]
	300 000	0.413[−02]	−0.141[−02]	0.776[−02]	−0.334[−02]
Perturbers are:		F III		F IV	
F V $3s$-$3p$	10 000	0.199[−03]	−0.115[−03]	0.179[−03]	−0.135[−03]
2455.0 Å	30 000	0.104[−02]	−0.521[−03]	0.110[−02]	−0.749[−03]
$C=0.22E+21$	50 000	0.186[−02]	−0.883[−03]	0.213[−02]	−0.131[−02]
	100 000	0.321[−02]	−0.154[−02]	0.416[−02]	−0.240[−02]
	200 000	0.459[−02]	−0.221[−02]	0.630[−02]	−0.357[−02]
	300 000	0.510[−02]	−0.262[−02]	0.753[−02]	−0.435[−02]
F V $3p$-$3d$	10 000	0.420[−03]	−0.126[−03]	0.380[−03]	−0.148[−03]
2701.6 å	30 000	0.206[−02]	−0.573[−03]	0.223[−02]	−0.823[−03]
$C=0.27E+21$	50 000	0.346[−02]	−0.976[−03]	0.406[−02]	−0.145[−02]
	100 000	0.550[−02]	−0.171[−02]	0.725[−02]	−0.267[−02]
	200 000	0.748[−02]	−0.248[−02]	0.104[−01]	−0.400[−02]
	300 000	0.811[−02]	−0.296[−02]	0.117[−01]	−0.489[−02]
Perturbers are:		F V		F VI	
F V $3s$-$3p$	10 000	0.163[−03]	−0.141[−03]	0.137[−03]	−0.131[−03]
2455.0 Å	30 000	0.113[−02]	−0.956[−03]	0.113[−02]	−0.114[−02]
$C=0.22E+21$	50 000	0.229[−02]	−0.173[−02]	0.238[−02]	−0.212[−02]
	100 000	0.481[−02]	−0.327[−02]	0.536[−02]	−0.417[−02]
	200 000	0.771[−02]	−0.507[−02]	0.911[−02]	−0.662[−02]
	300 000	0.972[−02]	−0.617[−02]	0.116[−01]	−0.811[−02]
F V $3p$-$3d$	10 000	0.345[−03]	−0.155[−03]	0.290[−03]	−0.144[−03]
2701.6 Å	30 000	0.230[−02]	−0.105[−02]	0.233[−02]	−0.125[−02]
$C=0.27E+21$	50 000	0.442[−02]	−0.191[−02]	0.466[−02]	−0.233[−02]
	100 000	0.856[−02]	−0.364[−02]	0.954[−02]	−0.463[−02]
	200 000	0.128[−01]	−0.569[−02]	0.149[−01]	−0.745[−02]
	300 000	0.152[−01]	−0.692[−02]	0.184[−01]	−0.911[−02]
Perturbers are:		F VII		F VIII	
F V $3s$-$3p$	100 000	0.100[−03]	−0.109[−03]	0.922[−04]	−0.106[−03]
2455.0 Å	30 000	0.113[−02]	−0.131[−02]	0.113[−02]	−0.145[−02]
$C=0.22E+21$	50 000	0.245[−02]	−0.250[−02]	0.250[−02]	−0.287[−02]
	100 000	0.585[−02]	−0.507[−02]	0.626[−02]	−0.590[−02]
	200 000	0.105[−01]	−0.827[−02]	0.119[−01]	−0.993[−02]
	300 000	0.135[−01]	−0.101[−01]	0.153[−01]	−0.121[−01]
F V $3p$-$3d$	10 000	0.212[−03]	−0.120[−03]	0.195[−03]	−0.117[−03]
2701.6 Å	30 000	0.234[−02]	−0.143[−02]	0.233[−02]	−0.159[−02]
$C=0.27E+21$	50 000	0.482[−02]	−0.276[−02]	0.494[−02]	−0.315[−02]
	100 000	0.104[−01]	−0.561[−02]	0.111[−01]	−0.653[−02]
	200 000	0.169[−01]	−0.926[−02]	0.190[−01]	−0.111[−01]
	300 000	0.212[−01]	−0.113[−01]	0.239[−01]	−0.135[−01]
Perturbers are:		S III		S IV	
F V $3s$-$3p$	10 000	0.222[−03]	−0.115[−03]	0.201[−03]	−0.135[−03]
2455.0 Å	30 000	0.114[−02]	−0.520[−03]	0.122[−02]	−0.748[−03]
$C=0.22E+21$	50 000	0.199[−02]	−0.878[−03]	0.230[−02]	−0.131[−02]
	100 000	0.332[−02]	−0.152[−02]	0.437[−02]	−0.237[−02]
	200 000	0.468[−02]	−0.216[−02]	0.646[−02]	−0.350[−02]
	300 000	0.514[−02]	−0.254[−02]	0.757[−02]	−0.423[−02]

TABLE I. (*Continued*.)

Perturber density=1×10^{17} cm^{-3}					
Perturbers are:		Electrons		Protons	
Transition	T (K)	Width (Å)	Shift (Å)	Width (Å)	Shift (Å)
F V $3p$-$3d$	10 000	0.469[−03]	−0.126[−03]	0.425[−03]	−0.148[−03]
2701.6 Å	30 000	0.225[−02]	−0.572[−03]	0.245[−02]	−0.823[−03]
$C=0.27E+21$	50 000	0.368[−02]	−0.970[−03]	0.437[−02]	−0.144[−02]
	100 000	0.570[−02]	−0.169[−02]	0.754[−02]	−0.263[−02]
	200 000	0.758[−02]	−0.242[−02]	0.107[−01]	−0.391[−02]
	300 000	0.822[−02]	−0.286[−02]	0.118[−01]	−0.476[−02]
Perturbers are:		S V		S VI	
F V $3s$-$3p$	10 000	0.182[−03]	−0.141[−03]	0.153[−03]	−0.131[−03]
2455.0 Å	30 000	0.125[−02]	−0.956[−03]	0.126[−02]	−0.114[−02]
$C=022E+21$	50 000	0.249[−02]	−0.172[−02]	0.261[−02]	−0.212[−02]
	100 000	0.510[−02]	−0.322[−02]	0.568[−02]	−0.411[−02]
	200 000	0.799[−02]	−0.493[−02]	0.936[−02]	−0.645[−02]
	300 000	0.985[−02]	−0.603[−02]	0.119[−01]	−0.789[−02]
F V $3p$-$3d$	10 000	0.386[−03]	−0.155[−03]	0.325[−03]	−0.144[−03]
2701.6 Å	30 000	0.254[−02]	−0.105[−02]	0.259[−02]	−0.125[−02]
$C=0.27E+21$	50 000	0.480[−02]	−0.190[−02]	0.508[−02]	−0.233[−02]
	100 000	0.903[−02]	−0.359[−02]	0.101[−01]	−0.457[−02]
	200 000	0.133[−01]	−0.554[−02]	0.155[−01]	−0.725[−02]
	300 000	0.154[−01]	−0.675[−02]	0.188[−01]	−0.888[−02]
Perturbers are:		S VII		S VIII	
F V $3s$-$3p$	10 000	0.112[−03]	−0.109[−03]	0.103[−03]	−0.106[−03]
2455.0 Å	30 000	0.126[−02]	−0.131[−02]	0.126[−02]	−0.145[−02]
$C=0.22E+21$	50 000	0.270[−02]	−0.250[−02]	0.276[−02]	−0.286[−02]
	100 000	0.621[−02]	−0.501[−02]	0.667[−02]	−0.585[−02]
	200 000	0.108[−01]	−0.807[−02]	0.122[−01]	−0.972[−02]
	300 000	0.138[−01]	−0.989[−02]	0.156[−01]	−0.119[−01]
F V $3p$-$3d$	10 000	0.238[−03]	−0.120[−03]	0.219[−03]	−0.117[−03]
2701.6 Å	30 000	0.260[−02]	−0.143[−02]	0.260[−02]	−0.159[−02]
$C=0.27E+21$	50 000	0.529[−02]	−0.275[−02]	0.543[−02]	−0.315[−02]
	100 000	0.110[−01]	−0.556[−02]	0.118[−01]	−0.648[−02]
	200 000	0.175[−01]	−0.906[−02]	0.196[−01]	−0.109[−01]
	300 000	0.217[−01]	−0.111[−01]	0.245[−01]	−0.133[−01]

shift along the S sequence ($4s'$-$4p'$ transition Cl II and Ar III) is detected [6]. This shift behavior was explained by the irregular change of the perturbing energy levels distribution around the upper level of the transition along the sequence. In this case simple theory [10] predicted the sign of the shift [6].

A general problem in the experimental studies along isoelectronic sequences is scaling of the data to the same temperature. Namely, experimental results for low ionization stages obtained at lower temperatures have to be compared with results for higher ionization stages measured at much higher temperatures. To perform a sensible comparison of the data along the sequence it is necessary to scale all experimental results to the same temperature. In cases when width or shift dependence upon temperature is not known this procedure may introduce an uncertainty in the comparison. Therefore the emphasis of this work is concentrated for several reasons on the temperature dependence of the Stark broadening parameters. Both experimental and theoretical investigations will be an extension of our study of $3s$-$3p$ and $3p$-$3d$ transitions of O IV [3] to N III and F V and it will be related to the recent study of the same transitions in another experiment performed with a different plasma source, diagnosed with another diagnostic technique [8].

II. THEORY

By using the semiclassical-perturbation formalism [11,12] we have calculated Stark broadening parameters for N III, O IV, and F V $3s^2S$-$3p(^1S)^2P^0$ and $3p^2P^0$-$3d(^1S)^2D$ multiplets. Besides electron impact line widths and shifts, Stark broadening parameters due to all relevant ion perturbers have been calculated as well. The corresponding data when perturbers are N II–N VI are calculated for N III multiplets and O III–O VI for O IV multiplets. Since in the case of the considered O IV transitions, several transitions between atomic energy levels with different parent terms may influence significantly, particularly on the shift values, the calculations with the inclusions of $2s2p(^3P^0)3p^2S$, $2s2p(^1P^0)3p^2S$, $2s2p(^3P^0)3p^2P$, $2s2p(^1P^0)3p^2P$, $2s2p(^3P^0)3p^2D$, $2s2p(^1P^0)3p^2D$, and $2p^2(^1D)3s^2D$ perturbing $2s^2(^1S)3p^2P^0$; transitions $2s2p(^3P^0)3s^2P^0$ and

$2s2p(^1P^0)3d^2P^0$ perturbing $2s^2(^1S)3d^2D$ and $2s2p(^1P^0)3s^2P^0$ perturbing $2s^2(^1S)3s^2S$ transitions have been performed here.

In order to assure the consistency of the data set, all oscillator strengths (and not only those for added transitions with different parent terms) have been taken from the TOP base (the complete package of the opacity project (OP) data with the database management system is usually referred to as TOP base) [13,14]. In order to compare experimental results for O IV lines from another experiment [8] performed in CO_2, the contribution of the C III–C V perturbers to the width of O IV multiplets are calculated as well. If one compares Stark widths and shifts for O IV calculated with the Coulomb oscillator strengths and oscillator strengths from the TOP base, one obtains for the $3s$-$3p$ multiplet at an electron density of 10^{17} cm^{-3} and $T=100\,000$ K, $w=0.0741$ Å and $d=-0.002\,40$ Å with Coulomb oscillator strengths and $w=0.0741$ Å and $d=-0.002\,33$ Å with TOP base oscillator strengths. For the $3p$-$3d$ multiplet one obtains $w=0.0784$ Å and $d=-0.002\,22$ Å and $w=0.0716$ Å and $d=-0.000\,955$ Å, respectively. If one adds the above mentioned transitions with different parent terms $w=0.0903$ Å and $d=+0.008\,03$ Å for the $3s$-$3p$ multiplet and $w=0.0824$ Å and $d=+0.007\,37$ Å for the $3p$-$3d$ multiplet. One can see that the influence of the perturbing levels with different parent terms is more significant than the differences between Coulomb and TOP base oscillator strengths. Since the measurements of F V Stark widths were performed in the mixture of SF_6 with He and in [8] SF_6 with hydrogen, Stark widths and shifts when S III–S VII and F III–F VII are perturbers have been calculated also. A summary of the formalism used for these calculations is given in [15].

Energy levels needed for calculations have been taken from [16]. For all radiators except O IV oscillator strengths were calculated by using the method by Bates and Damgaard [17,18]. We have been using the method described in Ref. [19] for higher energy levels. Our results are shown in Table I for a perturbers density of 10^{17} cm^{-3} and temperatures $T=10\,000$–$150\,000$ K for N III, O IV, and F V. We also specify a parameter C [15] which, when divided by the corresponding electron-impact full width at half maximum (FWHM), gives an estimate for the maximum perturbers density for which the line may be treated as isolated. For each value given in Table I the collision volume V multiplied by the perturbers density N is much less than one and therefore the binary approximation is valid. Since V is proportional to the cube of the typical emitter-perturber distance $\rho_{\rm typ}^3$, and $\rho_{\rm typ}^3$ may be estimated from the width, representing the width as proportional to the perturber density N, the average velocity v, and the average total cross section $\sigma_{\rm typ}$ ($\sigma_{\rm typ}=\pi\rho_{\rm typ}^2$), this is a good estimate of the validity of the impact approximation [15]. When the impact approximation is not valid, the ion-broadening contribution may be estimated by using quasistatic estimations [1,20]. In the significant parameter region in between where neither of these two approximations is valid, a unified type theory should be used. For example, in Ref. [21] simple analytical forms for such cases are given. The accuracy of the results obtained decreases when broadening by ion interaction becomes important. At high densities, the results are no longer linear with density due to the Debye screening. This effect is more important for the shifts than for the widths.

III. EXPERIMENT

The experimental apparatus and procedure are described in [3] so only minimum details will be given here. The light source was a low pressure pulsed arc with a quartz discharge tube 10 mm internal diameter. The distance between aluminum electrodes was 161 mm, and 3 mm diameter holes were located at the center of both electrodes to allow end-on plasma observations. A 30 mm diaphragm placed in front of the focusing mirror ensures that light comes from the narrow cone about the arc axis. All plasma observations are performed with 1 m monochromator with inverse linear dispersion 8.33 Å/mm in the first order of the diffraction grating, equipped with the photomultiplier tube and a stepping motor. The discharge was driven by a 15.2 μF low inductance capacitor charged to 3 kV (nitrogen experiment: peak current $I_p=14.8$ kA, critically damped current pulse duration $\tau=7.7$ μs, pressure of the gas mixture $p=3$ torr, continuous flow of the gas mixture, composition: 2.0% of N_2 in He) and to 4.8 kV (fluorine experiment: $I_p=20.5$ kA, $\tau=8.3$ μs, $p=0.8$ torr, continuous flow of the mixture 1.4% of SF_6 in He) and fired by an ignitron. The stepping motor and oscilloscope are controlled by a personal computer, which was also used for data acquisition. Recordings of spectral line shapes were performed shot by shot. At each wavelength position of the monochromator time evolution and decay of the plasma radiation were recorded by the digital oscilloscope. Four such signals were averaged at each wavelength. To construct the line profiles these averaged signals at different wavelengths and at various times of the plasma existence were used to construct line profiles. Spectral line profiles were recorded with instrumental half widths of 0.168 Å and 0.192 Å in nitrogen and fluorine experiments, respectively. To determine the Stark half width from the measured profile, a standard deconvolution procedure for the Lorentzian (Stark) and Gaussian (instrumental+Doppler) profiles [22] was used.

For the line-shift measurements we used line profiles at the different times of the plasma existence [23]. For this technique of shift measurements it is necessary to know plasma parameters (electron density and temperature) at the times when both profiles are recorded.

For the electron-density measurements we used, as in our oxygen experiment [3], the width of the He II P_α 4686 Å line [24]. Our main concern in the electron-density measurements was a possible presence of self-absorption of the P_α line which may distort the line profile. This would result in erroneous reading of the line width which would introduce an error in the electron-density measurements. In order to determine the optical thickness of the investigated lines we have introduced in the discharge an additional movable electrode [3,25]. By placing the movable electrode (10 mm thick) at two different positions and by recording the line profiles from two plasma lengths, it is possible to determine $\kappa_\lambda l$, where κ_λ is the spectral line absorption coefficient and l is the plasma length along the direction of observation. Since the measured $\kappa_\lambda l$ for the He II P_α line was always smaller than one it was possible to recover the line profile [26]. Great care was also taken to find the optimum conditions with the least self-absorption of the investigated lines. This was

TABLE II. Transition probabilities for the spectral lines used for the electron temperature measurements.

Ion	Wavelength (Å)	Transition	A (10^8 s^{-1})	Ref.
N III	4097.33	$3s^2S_{1/2}$-$3p^2P^0_{3/2}$	0.853	[28]
	4103.43	$3s^2S_{1/2}$-$3p^2P^0_{1/2}$	0.844	[28]
	4634.16	$3p^2P^0_{1/2}$-$3d^2D_{3/2}$	0.721	[28]
	4640.64	$3p^2P^0_{3/2}$-$3d^2D_{5/2}$	0.864	[28]
N IV	4057.80	$3p^1P^0_1$-$3d^1D_2$	0.662	[44]
F IV	2451.58	$3p^3D_2$-$3d^3F^0_3$	2.39	[45]
	2820.74	$3s^3P^0_1$-$3p^3D_2$	1.11	[45]
	2823.80	$3s^3P^0_0$-$3p^3D_1$	0.823	[45]
	2826.13	$3s^3P^0_2$-$3p^3D_3$	1.48	[45]
F V	2450.66	$3s^2S_{1/2}$-$3p^2P^0_{3/2}$	1.74	[28]
	2703.96	$3p^2P^0_{3/2}$-$3d^2D_{5/2}$	1.30	[28]

achieved by careful examination of the N III and F V line shapes as a function of the experimental conditions (total gas pressure, gas mixture composition, and condenser bank energy), and by checking the optical depth of the strongest lines by measuring the intensity ratios within multiplets and comparing them with theoretical predictions based on the L-S coupling (see, e.g., Ref. [27]). The ratios of N_2 and SF_6 in the mixture with helium were determined after a number of experiments in which these gases were diluted gradually until line intensities within investigated multiplets agree within 3% with the values derived from transition probabilities [28].

The axial electron temperatures were determined in the nitrogen-helium mixture from (a) the Boltzmann plot of the relative intensities of N III 4097.33, 4103.43, 4634.16, and 4640.64 Å lines and (b) from relative intensities of two lines 4097.33 and 4057.80 Å belonging to two successive ionization stages of nitrogen, N III and N IV, respectively. In the SF_6-helium mixture electron temperatures are determined (a) from a Boltzmann plot of F IV 2451.58, 2820.74, 2823.80, and 2826.13 Å lines and (b) from the relative intensities of the 2451.58, and 2450.66 Å lines belonging to F IV and F V, respectively. Transition probabilities and data sources for these measurements are given in Table II. The spectral response of the photomultiplier-monochromator system was calibrated against a standard coiled-coil quartz iodine lamp.

TABLE III. Experimental electron densities N_e and temperatures T_I and T_B derived from the relative intensities of the lines of successive ionization stages and from the Boltzmann plots of relative line intensities, respectively. Estimated uncertainties are given also.

Ion	t (μs)	N_e (10^{17} cm^{-3})	T_I (K)	R_B (K)
N III	1.5	1.38±15%	55 300	33 000±10%
	2.0	1.71±14%	59 300	36 100±10%
	2.5	2.52±14%	64 800	44 300±10%
	3.0	2.64±14%	70 500	39 600±10%
	6.0	1.11±15%	54 700	37 900±10%
F V	1.0	2.54±15%	89 900	71 200±12%

IV. RESULTS AND DISCUSSION

The experimental results for the electron densities and temperatures at the axis of the discharge at various times of the current pulse through the discharge tube are given in Table III together with estimated uncertainties. Since we have been studying Stark broadening parameters dependence upon temperature T_e we made an attempt to determine T_e as accurately as possible using two independent methods. Unfortunately, to apply a very sensitive method of the relative line intensities from two successive ionization stages one requires much higher plasma electron densities [see the local thermodynamic equilibrium (LTE) condition in Eq. (6.55) of Ref. [29]] than were available in our experiment, see Table III. Nevertheless both sets of electron temperatures are given in Table III. For obvious reasons only electron temperatures derived from the Boltzmann plots of the N III and F IV relative line intensities are given with estimated errors, see Table III, and they are used in further discussions. Here it should be pointed out that the possible presence of plasma inhomogeneity may influence electron temperature measurements considerably, namely, if the plasma is inhomogeneous the different ions will radiate primarily from different temperature regions and this can yield large errors in the temperature determination. In order to test the homogeneity of the observed plasma cone electron temperatures were determined with the different apertures of the optical system; observations were performed with a 3 cm and a 10 cm diaphragm in front the focusing mirror. This corresponds to the change of the diameter of the base of the observed plasma cone from 3.6 mm to 7.9 mm (internal diameter of the discharge tube is 10 mm). Within an experimental scatter of the temperature measurements in the time of interest no difference in T_e is detected.

The experimental results for the Stark widths (FWHM), of N III and F V lines are given in Table IV together with the estimated errors. Table IV also contains spectroscopic data for the investigated lines and comparisons with the semiclassical theoretical results obtained by using the semiclassical perturbation approach [11,12] with the code used in a number of papers by M. S. Dimitrijević and S. Sahal-Bréchot (see, e.g., Refs. [30–34]) denoted here as W_{DSB} (electron +ion impact widths, see Table I). Comparison is also made in the same table with theoretical results calculated after

TABLE IV. Experimental Stark widths w_m (FWHM) of investigated N III and F V lines from the $3s^2S$-$3p(^1S)^2P^0$ and the $3p^2P^0$-$3d(^1S)^2D$ multiplets are compared in this table with theoretical widths: semiclassical electron impact, w^e_{DSB}, electron+ion impact, w^{ei}_{DSB}, simplified semiclassical approach after Griem [Eq. (526) of Ref. [1]], w_G, and modified semiempirical formula after Dimitrijević and Konjević [35]. Theoretical widths w^e_{DSB} and w^{ei}_{DSB} are calculated from the data in Table I.

Ion	Transition	λ (Å)	N_e (10^{17} cm^{-3})	T_e (K)	w_m (Å)	w_m/W^e_{DSB}	w_m/w^{ei}_{DSB}	$w_m/_G$	w_m/w_{DK}
N III	$3s^2S_{1/2}$-$3p^2P^0{}_{3/2}$	4097.33	1.38±15%	33 000	0.34_5±7%	0.92	0.89	1.02	1.36
			1.71±14%	36 100	0.42_3±7%	0.93	0.91	1.05	1.40
			2.52±14%	44 300	0.55_7±6%	0.91	0.88	1.01	1.39
			2.64±14%	39 600	0.58_7±6%	0.88	0.85	0.98	1.33
			1.11±15%	37 900	0.26_2±6%	0.92	0.88	1.02	1.38
	$3s^2S_{1/2}$-$3p^2P^0{}_{1/2}$	4103.43	1.38±15%	33 000	0.34_3±7%	0.92	0.89	1.02	1.36
			1.71±14%	36 100	0.40_0±7%	0.90	0.87	1.00	1.32
			2.52±14%	44 300	0.55_7±5%	0.91	0.88	1.01	1.39
			2.64±14%	39 600	0.58_7±5%	0.88	0.85	0.98	1.33
			1.11±15%	37 900	0.27_9±8%	0.98	0.94	1.09	1.46
	$3p^2P^0{}_{1/2}$-$3d^2D_{3/2}$	4634.16	1.38±15%	33 000	0.47_0±7%	1.00	0.97	1.02	1.49
			1.71±14%	36 100	0.55_3±7%	0.97	0.94	0.99	1.46
			2.52±14%	44 300	0.76_6±6%	1.00	0.96	1.00	1.51
			2.64±14%	39 600	0.79_5±6%	0.95	0.91	0.96	1.44
			1.11±15%	37 900	0.35_2±8%	0.98	0.94	0.99	1.49
	$3p^2P^0{}_{3/2}$-$3d^2D_{5/2}$	4640.64	1.38±15%	33 000	0.443±7%	0.95	0.91	0.96	1.40
			1.71±14%	36 100	0.52_6±7%	0.94	0.90	0.95	1.41
			2.52±14%	44 300	0.74_6±5%	0.97	0.93	0.96	1.47
			2.64±14%	39 600	0.79_5±5%	0.95	0.91	0.96	1.44
			1.11±15%	37 900	0.35_2±8%	0.98	0.94	0.99	1.49
F V	$3s^2S_{1/2}$-$3p^2P^0{}_{3/2}$	2450.66	2.54±14%	71 200	0.11_6±5%	1.04	0.99	1.49	1.76
	$3p^2P^0{}_{3/2}$-$3d^2D_{5/2}$	2703.96	2.54±14%	71 200	0.13_4±5%	1.04	0.99	1.54	2.02

Griem [Eq. (526) in Ref. [1]] W_G, and results obtained after Dimitrijević and Konjević [35] W_{DK}. In order to evaluate the contribution of ion impact widths it was necessary to compute plasma composition data for the conditions of the width measurements (electron density and temperature). Here, to simplify calculations we assumed the LTE for our plasma conditions ($N_e > 10^{17}$ cm^{-3}) and the plasma composition data was evaluated as described for the LTE conditions in [29]. The assumption of the LTE conditions is obviously very crude (see two sets of results for electron temperatures in Table III). Its use may be justified by the fact that (a) the expected contribution of all ions in the plasma to the line width or shift may not exceed 10% of the electron width, see Table I, and (b) the difference in the contribution of various ions to the linewidths and shifts is so small (see Table I) that small differences in the computed concentrations of various ions in our experimental conditions is of marginal importance for the final result. For the computation of plasma composition data the energy levels necessary for evaluation of the partition functions are taken from [16,43]. Knowing the concentration of each type of the ion in the plasma, it is trivial (by the help of Table I) to estimate the ion contribution to the plasma broadened linewidth. This estimation is simplified by the fact that electron and ion impact widths have a Lorentzian shape, so the width of the profile represents the sum of the electron and all ion profiles.

The experimental shifts are given in Table V in the form $\Delta d_m/\Delta N_e$, so the estimated error also includes the uncertainty in the electron-density measurements. Since shifts are measured as a difference of two line profiles determined at two different times of the plasma existence corresponding plasma conditions N_e, T are also given in Table V. The experimental Stark shifts are compared with *our semiclassical results* (electrons and electrons+ions, see Table I) Δd_{DSB}, evaluated as for the widths. Since it is difficult to estimate plasma composition data in another experiment in order to estimate the contribution of ions, N III Stark shifts measured by Purić *et al.* [40] are compared in Table V only with our electron impact shifts.

To facilitate comparison between various experiments and theories all available results for studied N III and F V line widths are given in graphical form in Figs. 1–4. In these figures experimental widths are compared with (a) our semiclassical electron impact widths, (b) semiclassical electron impact widths calculated after Griem in [36], given only in Fig. 1, (c) simplified semiclassical results calculated here after Griem [Eq. (526) in Ref. [1]], and (d) modified semiempirical formula evaluated here after Dimitrijević and Konjević [35]. In addition, for our experimental conditions and for those in Ref. [8] plasma composition is evaluated and comparison with the semiclassical widths (electrons+ions) is performed.

Figure 1 shows N III for the $3s^2S$-$3p^2P^0$ multiplet. The large spread of the experimental data produces a very poor mutual consistency. Experimental results from Ref. [38] show large variations of linewidths within the multiplet which is usually an indication of the presence of self-absorption during line shape measurements (see also [36]). The large spread of the experimental widths in [39] may also be partially caused by the optical depth problem. If one takes

TABLE V. Experimental Stark shifts Δd_m determined as a wavelength shift between two lines profiles, compared with the corresponding theoretical shifts: electron impact, Δd^e_{DSB}, and electron+ion impact Δd^{ei}_{DSB}. Results for N III lines were calculated using Coulomb oscillator strengths while the results for O IV lines were obtained with TOP base oscillator strengths [13], [14] with transitions with different parent terms included (see Sec. II).

Ion	Transition	λ_{tab} (Å)	N_{e1} (10^{17} cm^{-3})	T_1 (K)	N_{e2} (10^{17} cm^{-3})	T_2 (K)	Δd_m (Å)	$\Delta d_m/\Delta d^e_{DSB}$	$\Delta d_m/\Delta d^{ei}_{DSB}$	Ref.
N III	$3s^2S_{1/2}$-$3p^2P^0_{3/2}$	4097.33	1.38	33 000	2.52	44 300	−0.04	5.6	7.4	[a]
	$3s^2S_{1/2}$-$3p^2P^0_{3/2}$	4097.33	∼0	∼0	1.78	50 000	−0.041	3.7	4.1	[40]
	$3s^2S_{1/2}$-$3p^2P^0_{1/2}$	4103.43	1.38	33 000	2.52	44 300	−0.04	5.6	7.4	[a]
	$3s^2S_{1/2}$-$3p^2P^0_{1/2}$	4103.43	∼0	∼0	1.78	50 000	−0.041	3.7	4.1	[40]
	$3p^2P^0_{1/2}$-$3d^2D_{3/2}$	4634.16	1.38	33 000	2.52	44 300	−0.04	5.4	8.3	[a]
	$3p^2P^0_{3/2}$-$3d^2D_{5/2}$	4640.64	1.38	33 000	2.52	44 300	−0.03	4.1	8.2	[a]
O IV	$3s^2S_{1/2}$-$3p^2P^0_{3/2}$	3063.43	2.06	62 600	5.07	93 600	0.03	1.4		[a]
	$3s^2S_{1/2}$-$3p^2P^0_{1/2}$	3071.60	2.06	62 600	5.07	93 600	0.03	1.4		[a]
	$3p^2P^0_{1/2}$-$3d^2D_{3/2}$	3403.60	2.06	62 600	5.07	93 600	0.03	1.5		[a]
	$3p^2P^0_{3/2}$-$3d^2D_{5/2}$	3411.76	2.06	62 600	5.07	93 600	0.03	1.5		[a]

[a]This work.

into account estimated experimental errors in Refs. [8], [37], and [39], all these results are in agreement with the present experiment. Spread of the experimental data, however, is rather large to make quantitative conclusions about the agreement with various theoretical approaches. Nevertheless, the best agreement is found with the semiclassical electron impact widths and the simple semiclassical formula [Eq. (526) of Ref. [1]].

Figure 2 shows N III, for the $3p^{2p0}-3d^2D$ multiplet. Comparison between the experimental results and theories is even more unclear. Three sets of experimental data [8], [37], and [39] are in good agreement with the modified semiempirical formula [35]. The present experiment, as in the preceding case, agrees best with our electron impact widths from Table I, and the simple formula [Eq. (526) in Ref. [1]].

Figure 3 shows F V, for the $3s^2S$-$3p^2P^0$ multiplet. Our experimental width is in very good agreement with the semiclassical data and lies between electron impact widths and

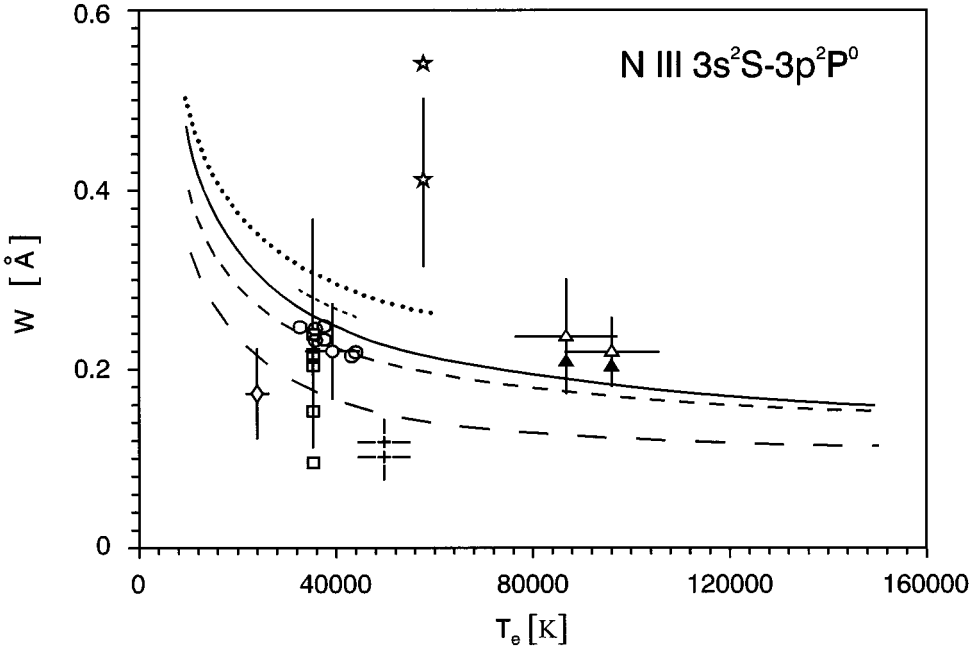

FIG. 1. Full Stark widths (normalized to an electron density of 10^{17} cm^{-3}) for the N III $3s^2S-3p^2P^0$ multiplet vs electron temperature. Theory: —, semiclassical, electron impact widths (see Table I); - - - - -, semiclassical, electron+ion impact widths (see Table I) evaluated only for the experimental conditions of this experiment; for the conditions of Ref. [8] theoretical electron+ion impact widths evaluated from Table I are denoted with Δ; ⋯, semiclassical, electron impact widths (after Griem [36]); – – –, simplified semiclassical approximation [after Griem, Eq. (526) of Ref. [1]]; and — — —, modified semiempirical formula (after Dimitrijević and Konjević [35]). Experiment: ○, this work, ◇, Popović, Platiša, and Konjević [31]; ☆, Källne, Jones, and Barnard [38]; □, Purcell and Barnard [39]; +, Purić, Srećković, Djeniže, and Platiša [40]; and △, Glenzer, Hey, and Kunze [8]. Estimated uncertainties of the experimental data are given whenever available in the original papers. Closed symbols denote theoretical widths (electrons+ions), open symbols denote experimental widths.

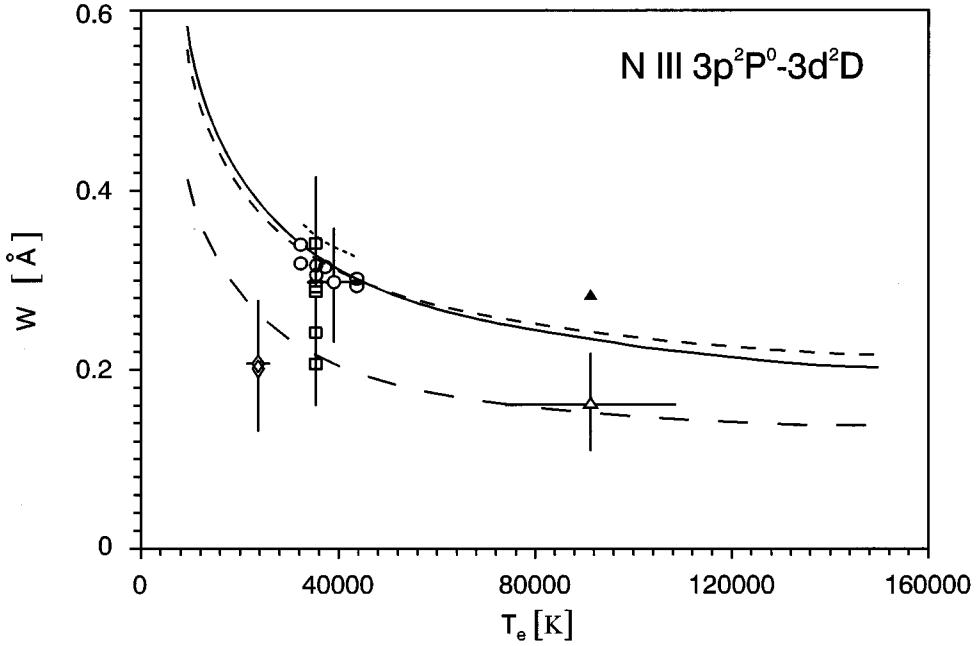

FIG. 2. Same as in Fig. 1 but for the N III $3p^2P^0$-$3d^2D$ multiplet.

electron+ion impact widths derived from data in Table I. The high temperature result of Glenzer, Heg, and Kunze [8], however, is much larger than all other theoretical results.

Figure 4 shows F V, for the $3p^2P^0$-$3d^2D$ multiplet. Both experimental results, this work and Ref. [8], are in very good agreement with our semiclassical data in Table I. On the basis of this result one may conclude that the semiclassical theory describes well the temperature dependence of the Stark widths. Unfortunately this conclusion may not be extended with such confidence to the other investigated multiplets.

Comparison of the N III experimental shifts shows reasonable agreement with our semiclassical results in spite of the fact that ratios of measured over theoretical values range from 1.8 up to 3.3 (see Table V). Measured shifts are very small in our experimental conditions and in this case accurate shift measurements are very difficult to perform. On the other side, theoretical results have a very large uncertainty

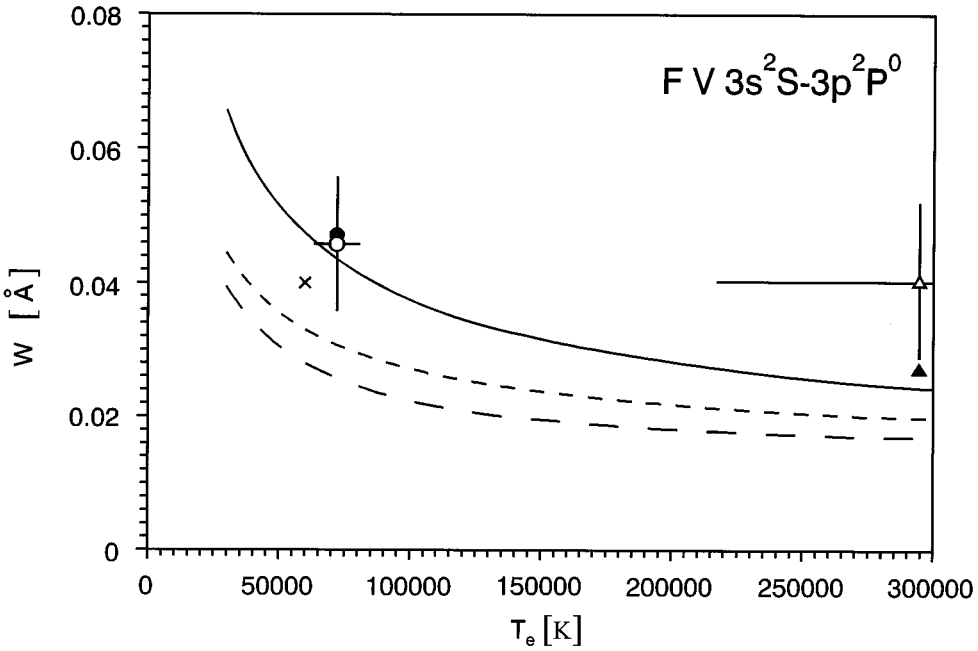

FIG. 3. Same as in Fig. 1 but for the *FV* $3s^2S$-$3p^2P^0$ multiplet; in addition, the predicted value *X*, derived from the regularity trend [47], is included.

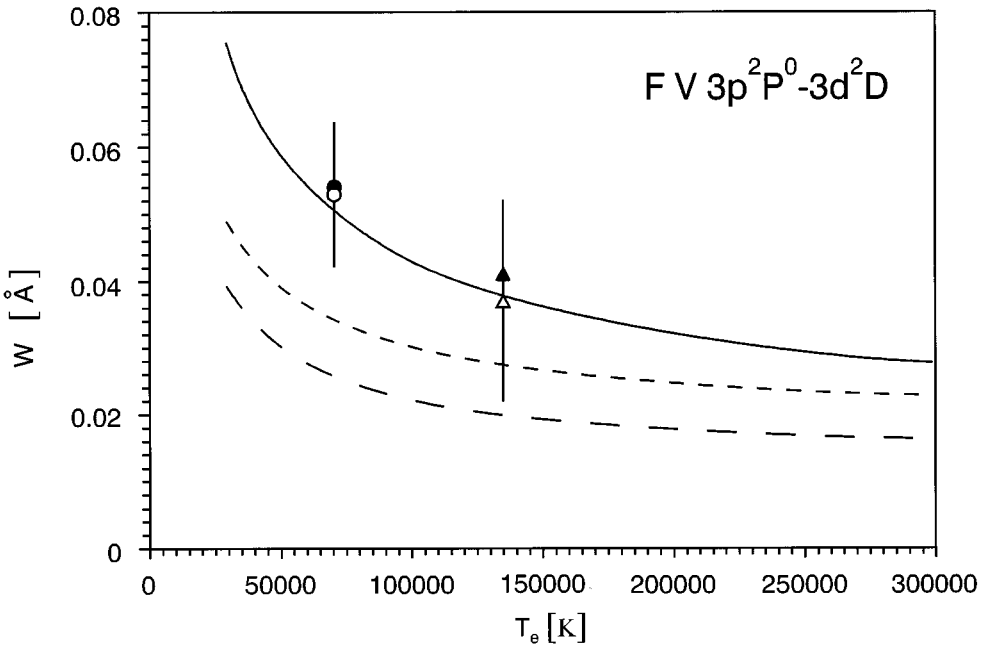

FIG. 4. Same as in Fig. 3 but for the $FV\ 3p^2P^0$-$3d^2D$ multiplet.

whenever shifts are small in comparison with widths as is the case with investigated N III and O IV lines, see Table I. Nevertheless, the results for N III lines of Purić *et al.* [40] agree better with our semiclassical results, see Table V. The agreement between theory and experiment for O IV lines is very good. Here we draw attention to the fact that, contrary to the blueshift of N III lines, O IV lines have a redshift, so good agreement with theoretical predictions is very encouraging. Once more we would like to stress that the use of perturbing energy levels with different parent terms in addition to those from allowed dipole transitions in our semiclassical calculations changed the direction of the shift of the O IV lines from blue to red (see Sec. II). Furthermore, from the comparison of the data in Table V one may conclude that the use of the theoretical ion impact shifts in addition to electron impact shift considerably improves the agreement between theory and experiment for both N III and O IV lines.

Finally, we made a comparison of the Stark widths along the isoelectronic sequence for both investigated multiplets, see Fig. 5. To perform this comparison it was necessary to normalize all experimental and theoretical results to the same temperature. Here we selected an electron temperature of 87 000 K (7.5 eV) which represent a medium value between the low and high temperature data and it was used for the same purpose in Ref. [8]. Temperature dependencies of our electron impact widths, see Table I and Table II in Ref. [3], are taken to normalize higher or lower temperature results. For clarity in comparison along the isoelectronic sequence only two sets of the most comprehensive results are used, this experiment together with Refs. [3] and [8], see Fig. 5. The relative position of the other experimental results can be determined from Figs. 1 and 2 and Figs. 2 and 3 of Ref. [3]. In Fig. 5 the theoretical dependencies of the Stark widths upon Z along the boron sequence are also introduced. Comparison of the experimental and theoretical data in Fig. 5 shows the following.

(a) The $3s^2S$-$3p^2P^0$ multiplet: with the exception of the F V experimental Stark width measured at a high temperature, 300 000 K [8] all other, lower temperature results agree, within the estimated uncertainties, with our semiclassical theoretical predictions. All simplified theoretical approaches show larger decrease of the Stark widths upon Z.

(b) The $3p^2P^0$-$3d^2D$ multiplet: with the exception of the N III Stark width from [8] all other experimental results agree with the semiclassical prediction. Although the simplified theoretical approach [Eq. (526), [1]] agrees best with experiments, the dependence upon Z is not correctly described as it is for the other simplified approaches [35] and [46].

It is common for the comparisons along the sequence for the widths of both multiplets that the agreement between our semiclassical results and experiment for the O IV lines improves if one takes into account the influence of the perturbing levels with the different parent terms.

V. CONCLUSIONS

The results of the semiclassical theoretical calculations for the Stark widths and shifts of N III and F V $3s^2S$-$3p^2P^0$ and $3p^2P^0$-$3d^2D$ multiplets have been reported. In addition to the electron impact widths and shifts, ion widths and shifts due to collisions with all ions of interest for our experimental conditions and those of Ref. [8] are calculated as well. Furthermore, for O IV lines, in addition to the data presented in [3], obtained with the LS coupling oscillator strengths, calculations by using the TOP base oscillator strengths (with and without inclusion of transitions with different parent terms) [13,14] and measured atomic energy levels [16] have been performed for the electronic and ionic perturbers. As-

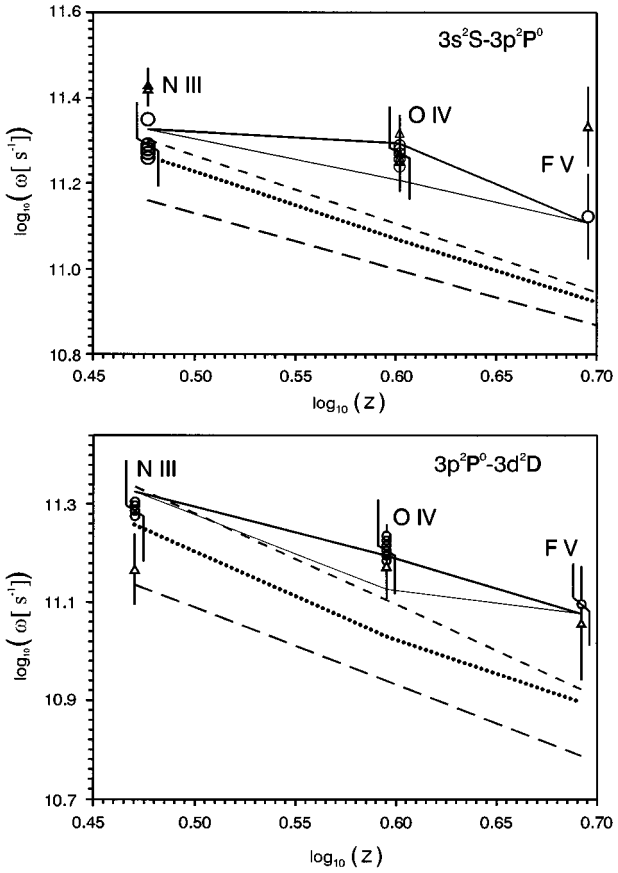

FIG. 5. Stark widths of the *B*-like spectral lines (in angular frequency units) as a function of $\log_{10}Z$. Experimental data are scaled linearly to a value of the electron density of 10^{17} cm^{-3} and to a value of the electron temperature 87 000 K (7.5 eV), Theoretical data are calculated for these values. Experimental results: △, Glenzer, Hey, and Kunze [8] and ○, this work. Error flags are calculated uncertainties including the error in the determination of the full width at half maximum and of the electron density measurements. Theoretical results: —, electron+ion impact widths, data for O IV lines with transitions with a different parent term (from Table I); —, electron+ion impact widths, data for O IV lines with transitions with a different parent term; ---, simple semiclassical, after Griem [Eq. (526) Ref. [1]]; – – –, modified semiempirical formula, after Dimitrijević and Konjević [35]; ⋯, classical-path approximation, after Hey and Breger [46] as calculated in Ref. [8].

suming plasma LTE conditions, plasma composition data are evaluated and, in conjunction with the results for the theoretical Stark broadening data, electron and ion impact widths and shifts are calculated. Experimental Stark widths of N III and F V lines and Stark shifts of N III and O IV lines of the same multiplets are measured in the plasma of a low pressure pulsed arc. Plasma electron density is determined from the width of He II P_α line while the electron temperatures are measured from the Boltzmann plot of the relative intensities of N III and F IV lines. Our experimental Stark widths are in agreement with most of the other experiments. The temperature dependence in the impact limit is characterized by two asymptotic regions and a rather narrow intermediate region. Basically they correspond to the elastic and inelastic collision regime. For neutral lines, the asymptotic analysis is presented, for example, in Refs. [41, 42]. For ions, however, such analysis is more complicated since the Stark broadening functions (A,a,B,b, see Ref. [1]) depend on two arguments and not on one as for neutrals. Consequently, an experimental investigation of the temperature dependence for ions is of higher interest. The temperature dependence of the experimental widths are best described with our semiclassical electron impact results, see Figs. 1–4. The high temperature result for the F V line of Ref. [8], see Fig. 3, represents an exception which cannot be explained within the uncertainty of the experiment and theory. Although we can conclude that all the simple formulas are in agreement with the experiments within their estimated uncertainties, which is typically about ±50%, Griem's simplified theoretical approach [Eq. (526) of Ref. [1]] agrees best with the experimental results, see Figs. 1–4, and Figs. 2 and 3 in Ref. [3].

Comparisons of the experimental widths along the isoelectronic sequence of boron in Fig. 5 show the best agreement with our semiclassical electron impact widths. Two exceptions are the $3p^2P^0$-$3d(^1S)^2D$ line of N III and, in particular, the high temperature result for the $3s^2S$-$3p(^1S)^2P^0$ line of F V, both results are from Ref. [8]. The inclusion of the oscillator strengths of the transitions with the different parent terms in the calculation of the widths of O IV lines improves the agreement between the theory and experiment. Although the simple formulas are in reasonable agreement with the experiments, none of them correctly describes $3p$-$3d$ Stark width dependence upon Z along the sequence, see Fig. 5.

Both measured experimental and calculated theoretical shifts for N III and O IV lines are very small and therefore their intercomparison under the present plasma conditions has a large uncertainty. Thus the agreement between semiclassical theory and this experiment can be considered satisfactory for N III lines, see Table V. The results for N III lines from another experiment [40] are in better agreement with our theory. For O IV lines, however, the experimental shifts have an opposite sign from the theoretically predicted ones [3]. An attempt has been made here to locate the cause of this discrepancy. It has been found that inclusion of ten transitions with different parent term improves the agreement between theory and experiment and correctly predicts a sign of the shift of the observed O IV lines.

Comparison of the data in Table V suggests that the ion impact shifts contribute considerably to the total theoretical shift of N III and O IV lines and its inclusion in the estimation of the total shift (electrons+ions) on the basis of the present experiment improves the agreement with the experiment. We cannot draw the same conclusion for the ion contribution to the Stark widths.

ACKNOWLEDGMENTS

The authors gratefully acknowledge the help of Dr. W. L. Wiese in selecting transition probabilities for the electron temperature measurements. This research is supported by the Ministry for Science and Technology of Serbia.

[1] H. R. Griem, *Spectral Line Broadening by Plasmas* (Academic, New York, 1974).
[2] N. Konjević and W. L. Wiese, J. Phys. Chem. Ref. Data **19**, 1307 (1990).
[3] B. Blagojević, M. V. Popović, N. Konjević, and M. Dimitrijević, Phys. Rev. E **50**, 2986 (1994).
[4] W. L. Wiese and N. Konjević, J. Quant. Spectrosc. Radiat. Transfer **28**, 185 (1982).
[5] F. Böttcher, P. Breger, J. D. Hey, and H.-J. Kunze, Phys. Rev. A **38**, 2690 (1988).
[6] R. Kobilarov and N. Konjević, Phys. Rev. A **41**, 6023 (1990).
[7] S. Glenzer, N. I. Uzelac, and H.-J. Kunze, Phys. Rev. A **45**, 8795 (1992).
[8] S. Glenzer, J. D. Hey, and H.-J. Kunze, J. Phys. B **27**, 413 (1994).
[9] W. L. Wiese and N. Konjević, J. Quant. Spectrosc. Radiat. Transfer **47**, 185 (1992).
[10] M. S. Dimitrijević and V. Kršljanin, Astron. Astrophys. **165**, 269 (1986).
[11] S. Sahal-Bréchot, Astron. Astrophys. **1**, 91 (1969).
[12] S. Sahal-Bréchot, Astron. Astrophys. **2**, 322 (1969).
[13] K. Butler, C. Mendoza, and C. J. Zeippen, J. Phys. B **26**, 4409 (1993).
[14] W. Cunto, C. Mendoza, F. Ochsenbein, and C. J. Zeippen, Astron. Astrophys. **275**, L5 (1993).
[15] M. S. Dimitrijević, S. Sahal-Bréchot, and V. Bommier, Astron. Astrophys. Suppl. Ser. **89**, 581 (1991).
[16] S. Bashkin and J. J. Stoner, Jr., *Atomic Energy Levels and Grotrian Diagrams* (North-Holland, Amsterdam, 1975), Vol. 1.
[17] D. R. Bates and A. Damgaard, Trans. R. Soc. London, Ser. A **242**, 101 (1949).
[18] G. K. Oertel and L. P. Shomo, Astrophys. J. Suppl. Ser. **16**, 175 (1968).
[19] H. Van Regemorter, Hoang Binh Dy, and M. Prud'homme, J. Phys. B **12**, 1073 (1979).
[20] S. Sahal-Bréchot, Astron. Astrophys. **245**, 322 (1991).
[21] A. J. Barnard, J. Cooper, and E. W. Smith, J. Quant. Spectrosc. Radiat. Transfer **14**, 1025 (1974).
[22] J. T. Davies and J. M. Vaughan, Astrophys. J. **137**, 1302 (1963).
[23] J. Purić and N. Konjević, Z. Phys. **249**, 440 (1972).
[24] T. L. Pittman and C. Fleurier, in *Proceedings of the Sixth International Conference on Spectral Line Shapes*, Boulder, 1982 (de Gruyter, Berlin, 1983).
[25] R. Kobilarov, N. Konjević, and M. V. Popović, Phys. Rev. A **40**, 3871 (1989).
[26] W. L. Wiese, in *Plasma Diagnostic Techniques*, edited by R. M. Huddleston and S. L. Leonard (Academic, New York, 1965).
[27] N. Konjević and W. L. Wiese, J. Phys. Chem. Ref. Data **5**, 259 (1976).
[28] S. Glenzer, H.-J. Kunze, J. Musielok, Y.-K. Kim, and W. L. Wiese, Phys. Rev. A **49**, 221 (1994).
[29] H. R. Griem, *Plasma Spectroscopy* (McGraw-Hill, New York, 1964).
[30] M. S. Dimitrijević and S. Sahal-Bréchot, Phys. Scr. (to be published).
[31] M. S. Dimitrijević, S. Sahal-Bréchot and V. Bommier, Astron. Astrophys. Suppl. Ser. **89**, 581 (1991).
[32] M. S. Dimitrijević, S. Sahal-Bréchot and V. Bommier, Astron. Astrophys. Suppl. Ser. **89**, 591 (1991).
[33] M. S. Dimitrijević and S. Sahal-Bréchot, Astron. Astophys. Suppl. Ser. **93**, 359 (1992).
[34] M. S. Dimitrijević and S. Sahal-Bréchot, Astron. Astrophys. Suppl. Ser. **95**, 109 (1992).
[35] M. S. Dimitrijević and N. Konjević, J. Quant. Spectrosc. Radiat. Transfer **24**, 451 (1980).
[36] M. S. Dimitrijević and N. Konjević, J. Quant. Spectrosc. Radiat. Transfer **25**, 387 (1981).
[37] M. V. Popović, M. Platiša, and N. Konjević, Astron. Astrophys. **41**, 463 (1975).
[38] E. Källne, L. A. Jones, and A. J. Barnard, J. Quant. Spectrosc. Radiat. Transfer **22**, 589 (1979); E. Källne and L. A. Jones *ibid*. **25**, 393 (1981).
[39] S. T. Purcell and A. J. Barnard, J. Quant. Spectrosc. Radiat. Transfer **32**, 205 (1984).
[40] J. Purić, A. Srećković, S. Djeniže, and M. Platiša, Phys. Rev. A **36**, 3957 (1987).
[41] S. A. Freudestein and J. Cooper, Astrophys. J. **224**, 1079 (1978).
[42] M. S. Dimitrijević and N. Konjević, Astron. Astrophys. **163**, 297 (1986).
[43] W. C. Martin, R. Zalubas, and A. Musgrove, J. Phys. Chem. Ref. Data **19**, 821 (1990).
[44] J. A. Tully, M. J. Seaton, and K. A. Berrington, J. Phys. B **23**, 3811 (1990).
[45] D. Luo and A. K. Pradham, J. Phys. B **22**, 3377 (1989).
[46] J. D. Hey and Breger, J. Quant. Spectrosc. Radiat. Transfer **24**, 349 (1980); **24**, 427 (1980); and J. D. Hey, S. Afr. J. Phys. **5**, 111 (1982).
[47] J. Purić, S. Djeniže, J. Labat, M. Platiša, A. Srećković, and M. Ćuk, Z. Phys. D **10**, 431 (1988).